Electron–Electron Double-Resonance Study of the Molecular Motion in End-Labeled Poly(styrene)

Henry W. H. Yang and James C. W. Chien*

Department of Chemistry, Department of Polymer Sciences and Engineering, and Materials Research Laboratories, University of Massachusetts, Amherst, Massachusetts 01003. *Received October 11, 1977*

ABSTRACT: The technique of frequency swept electron–electron double resonance (ELDOR) has been used to study polymer chain motions in dilute solutions. Optimum microwave power for the observing mode was determined from both the maximum ESR signal intensity and nearly constant ELDOR deenhancement. The latter was then measured as a function of microwave power for the pumping mode to obtain ELDOR deenhancement corresponding to infinite pumping power, R_m. Values of R_m for end-labeled poly(styrene) were obtained as a function of temperature for different ELDOR transitions. The results were analyzed by the Hyde–Chien–Freed ELDOR theory. From the theory correlation times were calculated which agree well with that obtained by ESR line width analysis. Both the activation energy (12 kJ mol^{-1}) and the correlation times of the motion were found to be significantly smaller than that obtained from other ESR and NMR studies on the aromatic substituted poly(styrene). The difference may be attributed to the smaller steric hindrance and less backbone coupling between neighboring bonds for the local motions of the polymer chain ends.

The technique of electron–electron double resonance (ELDOR[1]), in which a paramagnetic sample is irradiated simultaneously by two microwave frequencies differing in energy equal to the hyperfine separations of the ESR lines while observing energy transfer between the two microwave modes, has found interesting applications. A complex overlapping multiradical ESR spectra can be resolved and the structures of the free radicals can thus be identified as well as the nature of the relaxation processes.[2-4] Hyperfine couplings obscured by inhomogeneous broadening can also be determined with ELDOR.[5] Conformational changes arising from intramolecular rotational or torsional oscillatory motion in a solid or a single crystal[6-9] can also be studied with the ELDOR technique. For free radicals in solutions, it has been demonstrated that[1,2,10-13] the ELDOR technique is useful for the study of molecular motion with correlation times from 10^{-10} to 10^{-3} s. Especially in the slow-motional region between 10^{-7} to 10^{-3} s where ESR, NMR, and other techniques are insensitive to the motion, ELDOR offers a strong alternative means to characterize this molecular motion.

In order to fully exploit the unique capability of ELDOR in investigating molecular motions with long correlation times, the contributions of various molecular motions to the overall correlation time must be understood at short correlation times. Earlier,[13] we have presented ELDOR results on spin-labeled polymer samples. The purpose of the present work is to extend the measurements to allow extrapolation of ELDOR effects to infinite pump power and to analyze the data in terms of polymer chain dynamics. Yet another objective of this paper is to propose conditions for ELDOR experiments so that the results from different laboratories may be directly compared and related.

Experimental Section

Amorphous poly(styrene) (molecular weight 3×10^4) with nitroxide spin labels at both chain ends was a gift from Dr. P. M. Smith[14] of Aberdeen College. The synthesis and the characterization of this polymer has been given elsewhere.[15,16] This material is referred to as

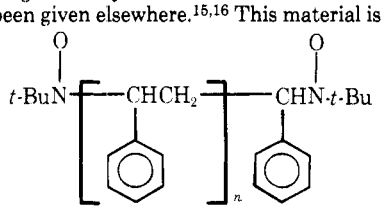

end-labeled poly(styrene). Also studied here are poly(styrene) labeled at the para position, heretofore referred to as ring-labeled poly(styrene).

Sample solutions were prepared by dissolving 6 wt % of polymer in tetrahydrofuran-d_8 with spin concentration ca. 1.5×10^{-4} M. Similar samples in protonated THF were also made. The solution was sealed in a quartz tube after a few freeze–pump–thaw cycle to remove oxygen from the solution. Both solutions give the same ELDOR effect in the temperature range studied.

The ELDOR effect was measured with a Varian E-800 frequency sweep ELDOR spectrometer. The cavity is a rectangular bimodal type.[1,17] A maximum of 1 W of klystron output can be delivered in the pump mode. ELDOR experiments were carried out by first turning off the pump mode and taking the ESR spectrum using the standard conditions. Then H_0 was adjusted to the position of the maximum in the derivative of the low-field ESR hyperfine line (see arrow mark in Figure 1a). The ELDOR bridge was then turned on with pump frequency, ν_p, adjusted to 25 MHz lower than ν_0, the observing frequency. After carefully maximizing the isolation between the pumping and the observing modes of the cavity, the ELDOR spectrum was then recorded while sweeping ν_p away from ν_0 until $\Delta\nu$ = 98 MHz (see Figure 1b). In all experiments, the modulation amplitude was chosen at ca. 0.25 of half-width of the observing hyperfine line, i.e., in the linear response region. Though little modulation frequency dependence of the ELDOR effect has been observed in our experiments, the modulation frequency was selected at 270 Hz in order to avoid the possible pseudorelaxation effect which arises when the modulation period is comparable to the electron spin–lattice relaxation time and artifacts due to rapid passage effect.[18,19] The reference phase was determined by adjusting to the maximum ESR signal intensity. The same phase setting was used throughout the ELDOR experiments.

The ELDOR effect is found to decrease to an asymptotic limit as the observing power is increased to saturate the ESR signal intensity (Figure 2). Therefore, the observing power was selected to obtain the maximum ESR signal (as indicated by the arrow in Figure 2). The ELDOR deenhancement value obtained under this condition is designated as R_s. It corresponds to a "saturation" condition as opposed to the condition of "no saturation" as reported in most of the ELDOR literature. The latter condition, being an ill-defined one, leads to results impossible to reproduce from laboratory to laboratory, or for the comparison of ELDOR effects at different temperatures. The temperature was controlled by using a Varian variable temperature controller with cooled nitrogen gas passed through the sample Dewer. A digital multimeter with a thermocouple was used to monitor the temperature; it was accurate to ±0.5 °C. In order to avoid an undesirable detector current drop in the low-temperature experiments at high pump powers, dry nitrogen gas was flushed continuously through the wave guides. Whenever there is a change in the detector current, the data were discarded.

The ELDOR effect is described by a reduction factor R as:

$$R = 1 - I/I_0 \qquad (1)$$

where I and I_0 are the observed ESR intensities with and without pumping.

Results and Discussion

Correlation Time for Spin-Labeled Poly(styrene) by ESR. The correlation time, τ, can be obtained from the ESR

0024-9297/78/2211-0759$01.00/0

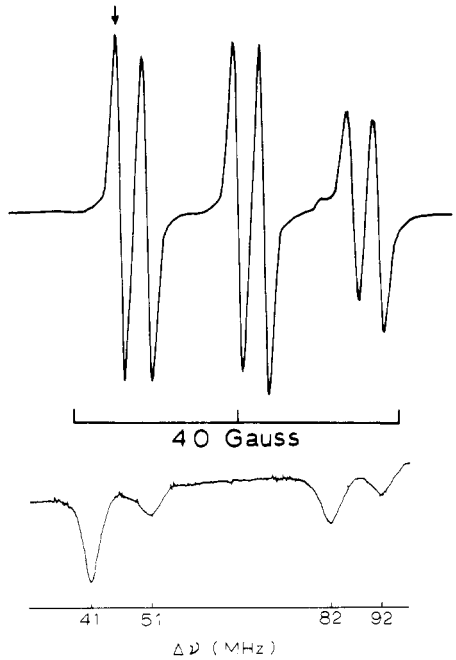

Figure 1. The ESR (top, a) and ELDOR (bottom, b) spectra of chain-end spin-labeled poly(styrene) in THF dilute solution at 25 °C.

spectrum directly. The ESR spectrum of end labeled poly(styrene) is shown in Figure 1a. The major hyperfine splitting is that with the ^{14}N nucleus (a_N = 41 MHz) and the minor splitting is that with the proton on the α carbon (a_H = 10 MHz). Following the method of Bullock et al.,[14,15] correlation times can be calculated from the relation:

$$\tau = \frac{23\nu(0)}{d^2}[S(+) + S(-) - 2] \qquad (2)$$

where $S(\pm) = [Y(0)/Y(\pm)]^{1/2}$, ν is the peak-to-peak line width, $d = \frac{2}{3}[A - \frac{1}{2}(B + C)]$, A, B, and C are the principal values of the hyperfine tensor (A = 90.8 MHz, B = 14.6 MHz, and C = 14.6 MHz), and Y is the peak-to-peak intensities of the relevant hyperfine line. The ^{14}N nuclear spin angular momenta $(m_I) = +1, 0, -1$ are denoted by (+), (0) and (−), respectively. The values of τ thus calculated are shown in Figure 2 as a function of temperature. By comparison, the end-labeled poly(styrene) has a much shorter correlation time than the ring-labeled specimen. They also differ in energies of activation which are 12 kJ mol^{-1} for end-labeled poly(styrene) and 19 kJ mol^{-1} for ring-labeled poly(styrene).

Effect of Microwave Power on ELDOR. The magnitude of the ELDOR effect is dependent on both the pumping and the observing microwave power. It will be very difficult to compare ELDOR results from different laboratories when the power levels are not specified. We propose here that all ELDOR deenhancements be extrapolated to infinite pump power with the strongly saturated observing mode as described below.

Hyde, Chien, and Freed[1] had shown the dependence of the ELDOR effect on the saturation parameters and pump power: (i) when the observing mode is "unsaturated":[20]

$$\frac{1}{R_u} = \frac{\Omega_p}{\Omega_{o,p}}\left[1 + \frac{1 + \Delta\omega_p^2 T_p^2}{T_p \Omega_p d_p^2}\right] \qquad (3)$$

(ii) when the observing mode is "strongly saturated":

$$\frac{1}{R_s} = \frac{\Omega_o + \Omega_{o,p}}{\Omega_{o,p}}\left[1 + \frac{\Omega_o(1 + \Delta\omega_p^2 T_p^2)}{T_p(\Omega_o^2 - \Omega_{o,p}^2 d_p^2}\right] \qquad (4)$$

where R_u and R_s are the ELDOR deenhancement factors for unsaturated and strongly saturated observing mode, respectively; Ω_o and Ω_p are the saturation parameters for the observed line and pump line, respectively; $\Omega_{o,p}$ is the cross-saturation parameter which leads to observable ELDOR effect; $\Delta\omega_p$ is the frequency deviation from resonance of the pump line; T_p is the transverse relaxation times for the pump mode; and $d_p^2 = \frac{1}{4}\gamma_e B_p^2$ (B_p is the circularly rotating component of pumping microwave magnetic field, and γ_e is the magnetogyric ratio of the electron). Since B_p^2 is proportional to P, the power incident on the cavity in the pump mode, eq 3 and 4, shows that $1/R$ follows a linear dependence upon $1/P$. The intercept is $1/R_m$ corresponding to infinite pump power. R_m bears a simple relationship to the saturation parameters and is independent of microwave power.[20]

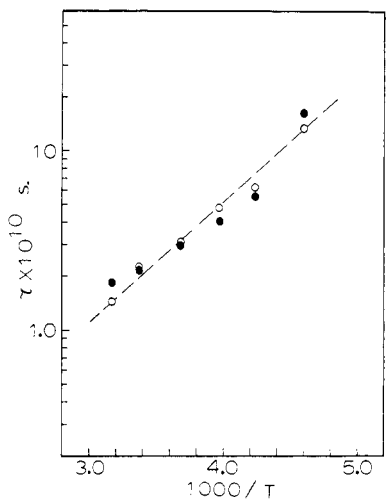

Figure 2. Arrhenius plot of the correlation times τ at various temperatures: (○) from ESR line-width analysis for end-labeled poly(styrene); (●) values derived from ELDOR experiments on end-labeled poly(styrene).

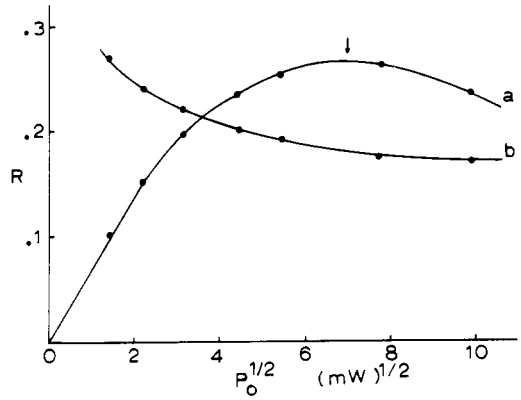

Figure 3. Dependences of ESR intensity (curve a, relative scale) and the ELDOR effect (curve b) on microwave power.

For each experiment the optimum microwave power for the observing mode is determined. This is done first for the ESR signal as shown in curve a of Figure 3 where the arrow indicates the optimum power level. Curve a is typical for inhomogeneously broadened ESR lines. Next the variation of ELDOR effect with observing power is determined. Figure 1b shows a typical ELDOR spectrum. The dependence is shown in Figure 3, curve b. The value of R decreases with an increase of observing power to a nearly constant value for observing power equal to or greater than the optimum level. Finally, with the observing mode set at this level, ELDOR spectra were obtained as a function of pump power. Figure 4 showed the linear dependence of $1/R$ vs. $1/P$ as required by eq 3 and 4.

ELDOR Effect for End-Labeled Poly(styrene). In these

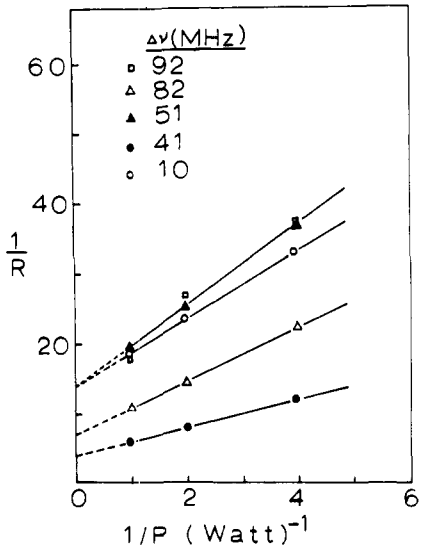

Figure 4. Dependence of the ELDOR effect on the pump power under a "strongly saturated" condition for end-labeled poly(styrene) in THF: 4.6×10^{-3} M, 43 °C.

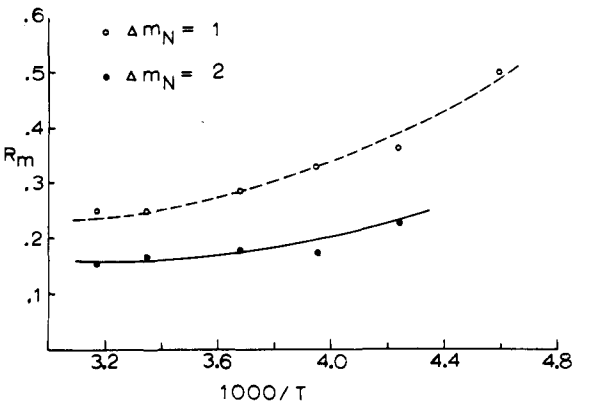

Figure 5. The temperature dependence of R_m: (○) $m_N = +1$ line being observed and $m_N = 0$ line being pumped; (●) $m_N = +1$ line being observed and $m_N = -1$ line being pumped. The experimental error is <±10%.

experiments the observing frequency always corresponds to that for the lowest field hyperfine line (as indicated by the arrow in Figure 1a). The ELDOR signals (Figure 1b) at $\Delta\nu$ = 10, 41, 51, 82, and 92 MHz correspond to pumping the (m_N, m_H) = (+1, −½), (0, +½), (0, −½), (−1, +½), and (−1, −½), respectively. The largest ELDOR effect occurs at $\Delta\nu$ = 41 MHz as expected from the selection rules of $\Delta m_N = \pm 1$, and $\Delta m_H = 0$ for electron–nuclear dipolar relaxation, END. In comparison, the ELDOR signal at $\Delta\nu$ = 82 MHz corresponding to $\Delta m_N = \pm 2$ and $\Delta m_H = 0$ has much smaller probability. The ELDOR signals at $\Delta\nu$ = 10, 51, and 92 MHz all require flipping of the proton spin; the magnitudes of these signals are all very small and about equal within experimental accuracy. The effect is unlikely due to the END process between the proton and the electron on nitrogen because of the large separation and the r^{-6} dependence for this process. More likely, relaxation occurs from interaction of the proton nuclear spin and the electron spin on the proton; there is a small unpaired spin density on the proton from hyperconjugation similar to the mechanism proprosed for β-proton coupling in proton magnetic resonance. All the low-temperature ELDOR effects were measured with observing power set for maximum ESR signal intensity. The temperature dependence of R_m is shown in Figure 5; R_m decreased to an asymptotic limit as the temperature decreases, and the differences for $\Delta m_N = 1$ and $\Delta m_N = 2$ ELDOR become less.

Relaxation Mechanisms for ELDOR Effect and Correlation Time Determined by ELDOR. The saturation parameters contain information about the electron spin transition, W_e, and the nuclear spin transition, W_N. At low temperatures W_N has been shown to be attributable[1] mainly to electron–nuclear dipolar interaction, W_N^{END}. This interaction is not the same for every hyperfine transition. The other mechanism which is important at the high-temperature region is the spin exchange (Heisenberg exchange, HE, and chemical exchange) with exchange frequency ω proportional to the spin concentration and temperature and inversely proportional to the solution viscosity.[1] This mechanism contributes approximately equally to ELDOR intensity independent of the difference between m_I of the pumped and the observed transitions. The transition probabilities W_N^{END} and W_e can be written as[1,21-23]

$$W_N^{END} = \frac{1}{10}\gamma_e^2\gamma_N^2\hbar^2 \sum_m (D_n{}^m D_n{}^{-m}) \frac{\tau}{1+\omega_N^2\tau^2} \quad (5)$$

$$W_e = \frac{\tau}{1+\omega_0^2\tau^2}\left\{\frac{13}{40}Z^2 + \frac{1}{40}\omega_0^2 \sum_i (g_i - g_s)^2\right\} + \frac{1}{18\tau}\sum_i (g_i - g_e)^2 \quad (6)$$

Equation 6 is the expression for spin–lattice relaxation resulting from modulation of hyperfine anisotropy, g anisotropy, and spin rotation. In the above expressions $D_n{}^m = 0$ for $m_I \neq 0$, and $\gamma_e\nu_n\hbar D_n{}^0 = (6\pi)^{1/2}[A - a)/2$, $a = (A + B + C)/3$, $Z = 2(A - B)/3$, g_e is the free electron g factor, $g_s = (g_{xx} + g_{yy} + g_{zz})/3$, where $g_{xx} = 2.0089$, $g_{yy} = 2.0061$, $g_{zz} = 2.0027$ for the di-*tert*-butyl nitroxide (DTBN) radical,[24] and ω_N and ω_0 are the nitrogen and the electron Zeeman frequencies, respectively. According to eq 3 and 4, R_m is a function of the saturation parameters only and can be expressed in terms of relaxation parameters b ($=W_N^{END}/W_e$) and b' ($=\omega_{HE}/W_e$).[1] Table I summarizes these relations for the case where both exchange and END mechanisms are operative.

The experimental ELDOR results for the "unsaturated" and "strongly saturated" observing conditions for the end-labeled poly(styrene) in THF solutions at 25 °C are given in Table II. The ELDOR effects can also be calculated from theory (Table I) if values of b and b' are known. To obtain these values we refer to the curve for $\Delta m_N = 2$ ELDOR in

Table I
ELDOR effect, R_m, under Various Observing Transition Conditions[a,b]

Line pumped	Line observed (+1)	
	Unsaturated	Strongly saturated
0	$\frac{(b+b')(b+3b'+1)}{(1+3b')(1+b')+b(b+4b'+2)}$	$\frac{(b+b')(b+3b'+1)}{(1+3b')(1+b')+b(b+4b'+3)+(b+b')(b+3b'+1)}$
−1	$\frac{(b^2+b')(3b'+1)}{(1+3b')(1+b')+b(b+4b'+3)}$	$\frac{(b^2+b')(3b'+1)}{(1+3b')(1+b')+b(b+4b'+3)+(b^2+b')(3b'+1)}$

[a] $b = W_n^{END}/W_e$, $b' = \omega/W_e$. [b] For END only, let $b' = 0$. For exchange only let $b = 0$.

Table II
Comparison between Experimental Data and Theoretical Calculations for the ELDOR Effect, R_m, of Poly(styrene) in THF, 25 °C

	Exptl R_m		Theoretical calc[a]	
$\Delta\nu$, MHz	Unsaturated	Strongly saturated	Unsaturated	Strongly saturated
10, 51, 92	0.11	0.07		
41 (Δm_n = 1)	0.38	0.25	0.43	0.27
82 (Δm_n = 2)	0.22	0.17	0.20	0.17

[a] Theoretical calculations based on $b' = 0.26$ and $b = 0.5$.

Figure 5. The R_m values approach a constant at high temperatures. According to theory, the dominant relaxation mechanism is via Heisenberg exchange and $b = 0$. Then from $R_m = b'(3b' + 1)/(1 + 2b')$, b' is found to be equal to 0.26, which is independent of temperature. Then for any other temperatures, the observed R_m together with $b' = 0.26$ enabled the calculation of b using the appropriate expression in Table I. For instance $b = 0.5$ at 25 °C. Even though the values of b and b' were obtained parametrically from one of the ELDOR transitions at "strongly saturated" observing condition, correct values of R_m can be calculated for the other transitions at both "strongly saturated" and "unsaturated" observing conditions. The agreement between theory and experiment is illustrated by the results at 25 °C in Table II. Equally satisfactory agreements were found for all other temperatures, demonstrating the capability of the HCF theory[1] in predicting the ELDOR effect within experimental error.

Calculation of τ is achieved by solving eq 5 and 6 using the values of b and the known g and hyperfine anisotropies of the spin label (vide supra). This was done as a function of temperature and shown as filled circles in Figure 3. The correlation times obtained thusly are in good agreement with those obtained from ESR line width analysis.

Molecular Chain Dynamics. Figure 2 showed that the end-labeled poly(styrene) has a shorter correlation time than the ring-labeled poly(styrene). For instance at room temperature, τ is about 2.2×10^{-10} s for the end-labeled poly(styrene) as compared to 5.5×10^{-10} s for ring-labeled polymer. They also differ in activation energies; it is 12 and 19 kJ mol^{-1} for the end-labeled and ring-labeled poly(styrene), respectively. It is apparent that a spin label situated at the chain end experiences less steric hindrance against rotation or other segmental motion; it is not strongly coupled to the motion of neighboring bonds. There have been reports on other studies of molecular motion of poly(styrene) and its derivatives. Earlier dielectric[27,28] and recent NMR relaxation studies[29] on poly(*p*-fluorostyrene) and poly(*p*-chlorostyrene) found an activation energy of about 22 kJ mol^{-1}. Table III summarizes some of the previous studies on local motion of poly(styrene) and compares them with our present results. A more complete review of the local motion of poly(styrene) is available.[29]

The effect of molecular weight on the poly(styrene) chain motion has been explored in many previous studies.[14,29,30] Briefly, two classes of polymer chain motion may be observed for a polymer dissolved in a dilute solution: (a) local segmental motion characterized by a correlation time τ_c involving only a few neighboring repeating units and independent of polymer chain length; (b) rotational diffusion motion of the entire molecule which is strongly dependent on molecular weight and can be characterized by a correlation time τ_R represented as[14,29]

$$\tau_R = 2M[\eta]\eta_0/3RT \quad (7)$$

Table III
Correlation Times and Activation Energies for Local Chain Motion in Poly(styrene)

Method	Temp, °C	Solvent	τ, ps	E_a, kJ/mol
ESR[15]	30	Toluene	550	18
^{13}C NMR[29]	42	C_2Cl_4	600	
Raman line shape analysis[30]	25	CCl_4	400	
^{19}F NMR[28]	25	$CDCl_3$	240	22
ESR[a]	25	THF	35	12
ELDOR[a]	25	THF	38	12

[a] End-labeled poly(styrene).

where M is the molecular weight, $[\eta]$ is the intrinsic viscosity of the solution, and η_0 is the viscosity of the solvent at temperature T. These two types of motion are in competition with each other but only the resultant of them is observed. A simple way to represent this competing process is to let

$$1/\tau = 1/\tau_R + 1/\tau_c \quad (8)$$

where τ is the correlation time obtained from experiments. At sufficiently low molecular weight such that $\tau_R \ll \tau_c$, the molecular tumbling motion dominates the relaxation process. At this limit, the activation energy obtained by plotting ln τ vs. $1/T$ gives approximately the activation energy for viscous flow of the pure solvent which is 7.5 kJ mol^{-1} for THF. As the molecular weight of the compound increases, the activation energy obtained by the same procedure will also increase reaching finally a limiting value when $\tau_R \gg \tau_c$. The activation energy at this limit represents the barrier for local segmental motions described by the local correlation time.

The intrinsic viscosity $[\eta]$ of the chain-end labeled poly(styrene) in THF solution at 25 °C is 0.355 dL/g which does not vary significantly over the temperature range of our experiments. The rotational diffusion correlation time τ_R calculated from eq 7 is equal to 5.64×10^{-7}, 2.70×10^{-7}, and 1.05×10^{-7} s at −56, −20, and 43 °C, respectively. These values are more than three orders of magnitude larger than τ obtained from experiments. Thus, the difference between τ and τ_c, the corrected correlation time for local motion, is negligible. Therefore, the activation energy of 12 kJ mol^{-1} must be the energy barrier for the local segmental motion.

References and Notes

(1) J. S. Hyde, J. C. W. Chien, and J. H. Freed, *J. Chem. Phys.*, **48**, 4211 (1968).
(2) C. Mottley, K. Chang, and L. D. Kispert, *J. Magn. Reson.*, **19**, 130 (1975).
(3) J. S. Hyde, L. D. Kispert, R. C. Sneed, and J. C. W. Chien, *J. Chem. Phys.*, **8**, 3824 (1968).
(4) A. Lund, T. Gillbro, D.-F. Feng, and L. Kevan, *J. Chem. Phys.* **7**, 414 (1975).
(5) J. S. Hyde, R. C. Sneed, and G. H. Rist, *J. Chem. Phys.*, **51**, 1404 (1969).
(6) L. D. Kispert and K. Chang, and C. M. Bogan, *J. Chem. Phys.*, **58**, 2164 (1973).
(7) L. D. Kispert and K. Chang, *J. Magn. Reson.* **10**, 162 (1973).
(8) L. D. Kispert, K. Chang, and C. M. Brogan, *J. Phys. Chem.*, **77**, 629 (1973).
(9) L. D. Kispert and P. S. Wang, *J. Phys. Chem.*, **78**, 1839 (1974).
(10) G. V. Bruno and J. H. Freed, *Chem. Phys. Lett.*, **25**, 328 (1974).
(11) M. D. Smigel, L. R. Dalton, J. S. Hyde, and L. A. Dalton, *Proc. Natl. Acad. Sci. U.S.A.*, **71**, 1925 (1974).
(12) J. S. Hyde, M. D. Smigel, L. R. Dalton, and L. A. Dalton, *J. Chem. Phys.*, **62**, 1655 (1975).
(13) M. M. Dorio and J. C. W. Chien, *Macromolecules*, **8**, 734 (1975).
(14) A. T. Bullock, G. G. Cameron, and P. M. Smith, *J. Phys. Chem.*, **77**, 1635 (1973).
(15) A. T. Bullock, J. H. Butterworth, and G. G. Cameron, *Eur. Polym. J.*, **7**, 445 (1971).
(16) G. Drefahl, H.-H. Hörhold, and K. D. Hofmann, *J. Prakt. Chem.*, **37**, 137 (1968).

(17) L. Kevan and L. D. Kispert, "Electron Spin Double Resonance Spectroscopy", Wiley, New York, N.Y., 1976.
(18) M. M. Dorio and J. C. W. Chien, *J. Chem. Phys.*, **62**, 3963 (1975).
(19) J. S. Hyde and L. A. Dalton, *Chem. Phys. Lett.*, **16**, 568 (1972).
(20) M. P. Eastman, G. V. Bruno, and J. H. Freed, *J. Chem. Phys.*, **52**, 321 (1970).
(21) D. Kivelson, *J. Chem. Phys.* **33**, 1094 (1960); A. D. McLachlan, *Proc. R. Soc. London, Ser. A*, **280**, 271 (1964).
(22) P. W. Atkins and D. Kivelson, *J. Chem. Phys.*, **44**, 169 (1966).
(23) G. Nyberg, *Mol. Phys.*, **12**, 69 (1967).
(24) O. H. Griffith, D. W. Cornell, and H. M. McConnell, *J. Chem. Phys.*, **43**, 2909 (1965).
(25) From the exchange dominated ELDOR reduction factor, one can calculate the translational correlation time of the molecule.[26]
(26) E. Stetter, H.-M. Vieth, and K. H. Hausser, *J. Magn. Reson.*, **23**, 493 (1976).
(27) W. H. Stockmayer, *Pure Appl. Chem.*, **15**, 539 (1967).
(28) B. Baysal, B. A. Lowry, H. Yu, and W. H. Stockmayer, "Dielectric Properties of Polymers", F. E. Karasz, Ed., Plenum Press, New York, N.Y., 1971.
(29) K. Matsuo, K. F. Kuhlmann, H. W. H. Yang, F. Geny, and W. H. Stockmayer, *J. Polym. Sci., Polym. Phys. Ed.*, **15**, 1347 (1977).
(30) A. Allerhand and R. K. Hailstone, *J. Chem. Phys.*, **56**, 3718 (1972).
(31) H. Nomura and Y. Mayahara, *Polym. J.*, **8**, 30 (1976).

Long-Range Steric Effects on the Carbon-13 Chemical Shift of Hydrocarbon Polymers

L. Zetta, G. Gatti, and G. Audisio*

Istituto di Chimica delle Macromolecole del CNR, Via Alfonso Corti 12, 20133 Milano, Italy. *Received September 13, 1977*

ABSTRACT: High-resolution ^{13}C NMR was used to determine the microstructure of polymers having monomer units with a length of four atoms by exploiting long-range steric effects. In *trans*-1,4-polypentadiene the methyl absorption is affected by the triad steric sequence and the CH by the diad sequence. In *cis*-1,4-polypentadiene the *mm* and *rr* triads can be distinguished in the methyl absorption while the *m* and *r* diads are revealed by the CH and CH_2 signals. Finally the poly(1-methyltetramethylene) shows fine structure both in the methyl and in the β-CH_2 absorption which is attributed to triads and possibly to higher sequences.

I. Introduction

In recent years ^{13}C NMR spectroscopy has been largely applied to the study of the structure of both homo- and copolymers of hydrocarbon type, with particular reference to the determination of stereoregularity and monomer unit sequences.

This method is especially powerful in the study of the saturated carbon region because of the high sensitivity of the ^{13}C chemical shift to structural features. The correlation between chemical shift and chemical structure of the paraffinic hydrocarbons has been observed and rationalized by Grant and Paul[1] and later refined by Lindeman and Adams.[2] Both these empirical schemes are based on the substituent effect which a carbon atom has on the shift of the observed carbon. This effect has been observed for carbons placed in position α, β, γ, δ, and ϵ relative to the observed carbon. Subsequently it has been reported that the substituent effect is also related to steric structure.[3]

Correspondingly in the determination of microtacticity of polymers the ^{13}C method has been applied only to polymers having monomer units with length of two atoms (e.g., vinyl polymers)[4] or three atoms (e.g., polypropylene sulfide[5] and oxide[6]).

Of course the limitation of the method arises from the rapid attenuation of the substituent effect with distance, an effect which is of the δ type in the vinyl polymers and of the ϵ type in the other mentioned class of polymers.

The present work was undertaken with the aim of using the ^{13}C technique for determining triad sequences of polymers having monomer units with a length of four atoms, i.e., poly(1-methyltetramethylene) and 1,4-polypentadiene, exploiting the long-range stereospecific effect of a ζ methyl substituent on the chemical shift of the methyl group:

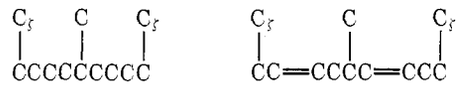

The ζ effect shows up in the spectrum of polypropylene[7,8] in the fine structure of the methyl signal due to steric pentads. This spectrum has been assigned[9] with the aid of model compounds and rationalized[10] in conformational terms.

Considering that in the case of poly(1-methyltetramethylene) the overall chain conformation could be different because of the absence of the δ-methyl group, it seemed interesting to determine whether the ζ effect was observable even in this case.

Concerning unsaturated polymers such as the 1,4-polypentadienes there is not available in the literature any method for the quantitative evaluation of their tacticity index. For example X-ray and IR spectroscopy gave evidence[11–13] of the iso or syndiotactic structure of 1,4-polypentadiene without providing a determination of the amount of stereoregular structure.

Moreover by ^{13}C spectroscopy it was possible to characterize cis and trans stereoisomeric polypentadienes as well as 1,2 and 1,4 structures but not iso and syndiotactic stereoisomer in 1,4 structures.[14]

Thus the present investigation was undertaken also in view of the possible interest of quantitatively knowing the steric composition of substituted dienic polymers, which may be useful for studies of their polymerization mechanism.

II. Experimental Section

1. Materials. Isotactic *trans*-1,4-polypentadiene (I) was prepared[15] by γ irradiation of the inclusion compound between deoxycholic acid and *cis*-1,3-pentadiene. The sample studied had an optical activity corresponding to $[\alpha]^{25}_D$ −21°.

Isotactic *trans*-1,4-polypentadiene (II) was prepared[16] by γ irradiation of the inclusion compound between perhydrotriphenylene and *trans*-1,3-pentadiene.

Isotactic *cis*-1,4-polypentadiene (III) was obtained by using the catalytic system:[17] 0.08 mL of titanium tetraisopropylate and 0.3 mL of $(C_2H_5)_3Al$ in 13.3 mL of dry benzene. The monomer was 2.5 mL of *trans*-1,3-pentadiene.

Syndiotactic *cis*-1,4-polypentadiene (IV) was prepared[18] by adding to 10 mL of dry benzene, 0.002 mL of H_2O, 0.09 g of $(C_2H_5)_2$-

0024-9297/78/2211-0763$01.00/0